

## Intramolecular Charge-Transfer Interactions in $\pi$ -Extended Tetrathiafulvalene Derivatives

Emad Aqad,<sup>†</sup> M. V. Lakshmikantham, Michael P. Cava, and Robert M. Metzger\*

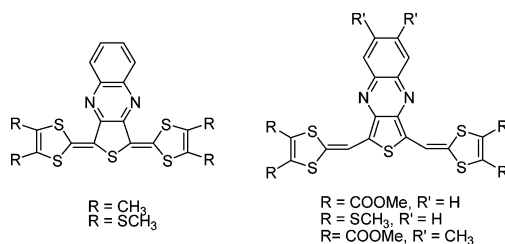
Department of Chemistry, The University of Alabama, Box 870336, Tuscaloosa, Alabama 35487-0336

Vladimir Khodorkhovskiy<sup>‡</sup>

Department of Chemistry, Ben Gurion University of the Negev, POB 653, Beer Sheva 84105, Israel

rmetzger@bama.ua.edu

Received June 24, 2004



New electron-donor (D)–electron-acceptor (A) TTF architectures are presented in which two electron-donating 1,3-dithiole moieties are connected by a  $\pi$  bridge to the weak electron-accepting quinoxaline moiety (D- $\pi$ -A compounds **9a** and **9b** and also two 1,3-dithiole-2-ylidene moieties are connected by a  $\pi$  bridge to the electron-accepting thieno[3,4-*b*]quinoxaline bridge (D- $\pi$ -A- $\pi$ -D compounds **12a–c**). There are through-bond intramolecular charge-transfer (ICT) interactions, predicted in theoretical calculations, and confirmed by UV–vis spectroscopy and cyclic voltammetry measurements. This work constitutes the first use of quinoxalines as electron-accepting moieties in D- $\pi$ -A compounds.

### Introduction

The impetus to the search for organic *intermolecular* charge-transfer complexes (CTC) came in the early seventies, with the discovery of one-dimensional conductivity exhibited by a charge-transfer complex, formed between the electron-donor (D) tetrathiafulvalene (TTF, **1**) and the electron-acceptor (A) 7,7,8,8-tetracyanoquinodimethane (TCNQ, **2**).<sup>1,2</sup> Since then, hundreds of variations on the basic structure of TTF molecule have been carried out, while considerably fewer variations on the structure of TCNQ were possible. Tremendous progress has been made within the fields of physical and theoretical chemistry toward designing and exploring the potential of TTFs as building blocks for materials with unique physical properties.<sup>3–6</sup> In this regard, the potential of the

TTF donating core, as a building block for conjugated D- $\pi$ -A molecular systems, is currently being explored.<sup>4,6,7</sup> The aim of D- $\pi$ -A systems is to obtain compounds that do not have the same characteristics as the parent donor and acceptor components. These delocalized  $\pi$ -electron systems are being explored, within the wide fields of nonlinear optics and solvatochromism, among others.

The synthesis of extended  $\pi$ -donors, in which the two 1,3-dithiole units of a TTF molecule are separated by one or more olefinic or quinonoid units, has been the subject of major research programs in our groups for several years. Previously, we reported the synthesis of the *p*-quinobis(benzo-1,3-dithiole) **3**,<sup>8</sup> TTF-vinylogues of general structure **4**,<sup>9–12</sup> and TTF-vinylogues in which the central double bond is replaced by a common heteroar-

<sup>†</sup> Present address: Department of Chemistry, University of Pennsylvania, 231 S. 34th St., Philadelphia, PA 19104-6323.

<sup>‡</sup> Present address: UMR 6114, Faculté des Sciences de Luminy, Université de la Méditerranée, Case 901, 13288 Marseille cedex 9, France.

(1) Ferraris, J. P.; Cowan D. O.; Walatka, V., Jr.; Perlstein, J. H. *J. Am. Chem. Soc.* **1973**, *95*, 948.

(2) Coleman, L. B.; Cohen M. F.; Sandman, D. J.; Yamagishi, F. G.; Garito A. F.; Heeger, A. J. *Solid State Commun.* **1973**, *12*, 1125.

(3) Metzger, R. M. *Chem. Rev.* **2003**, *103*, 3803.

(4) Segura, J. L.; Martin, N. *Angew. Chem., Int. Ed.* **2001**, *40*, 1372.

(5) Bryce, M. R. *J. Mater. Chem.* **2000**, *10*, 589.

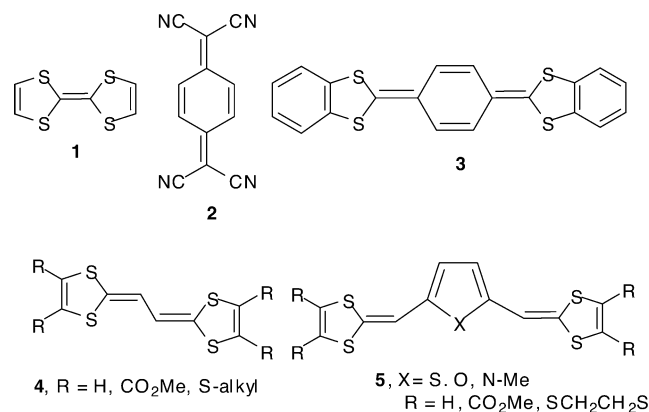
(6) Bryce, M. R. *Adv. Mater.* **1999**, *11*, 11.

(7) Aqad, E.; Ellern, A.; Shapiro, L.; Khodorkovskiy, V. *Tetrahedron Lett.* **2000**, *41*, 2983.

(8) Sato, M.; Lakshmikantham, M. V.; Cava, M. P.; Garito, A. F. *J. Org. Chem.* **1978**, *43*, 2084.

(9) Khodorkovskiy, V. Y.; Veselova, L. N.; Neilands, O. Ya. *Khim. Geterotsikl. Soedin.* **1990**, 130.

## CHART 1



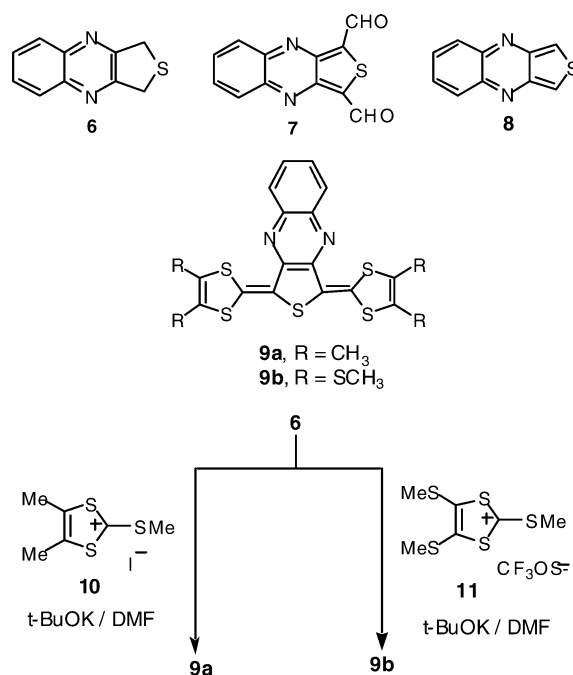
matic ring (structure **5**) (Chart 1).<sup>13</sup> Many papers describe the synthesis and properties of various  $\pi$ -extended TTF-based systems.<sup>14</sup> In general, vinylogues of TTF are characterized by a fairly low first oxidation potential and a smaller difference between the first and the second oxidation potentials.<sup>15</sup> This tuning of the redox properties of extended-TTF  $\pi$ -donors is attributed to an increased delocalization of the positive charge in the singly oxidized cation and a reduced Coulomb repulsion within the doubly oxidized dication.

In our recent paper, we reported that stable hetero-[3,4-*b*]quinoxaline derivatives are strong electron acceptors.<sup>16</sup> Here, we report the use of such electron-deficient and electroactive compounds as components for D- $\pi$ -A molecular systems. In particular, we prepared several new TTF  $\pi$ -extended systems which incorporate dihydrothieno[3,4-*b*]quinoxaline or thieno[3,4-*b*]quinoxaline electron-accepting moieties in the bridge and studied how the bridging of the two 1,3-dithiole units by an electron-accepting moiety affected the physical and chemical properties of such systems.

## Results and Discussion

**Synthesis.** The key starting materials for the synthesis of the new compounds were 1,3-dihydrothieno[3,4-*b*]quinoxaline (**6**) and 1,3-diformylthieno[3,4-*b*]quinoxaline (**7**). In our ongoing studies of heteroaromatic *o*-quinonoid heterocycles, we previously reported the synthesis of thieno[3,4-*b*]quinoxaline (**8**),<sup>17</sup> which was obtained as an acid-sensitive compound and which was stable for several days in the dark. In contrast, the 1,3-diformyl derivative **7** was found to be very stable.<sup>17</sup> We also reported that compound **6** reacts with aromatic aldehydes in a Knoevenagel reaction, with the formation of unsaturated

## SCHEME 1



condensation products.<sup>17</sup> We attributed the special reactivity of **6** to the electron-withdrawing effect of the pyrazine ring, which is condensed to the 3- and 4-positions of the thiophene ring. Similar behavior was observed for 1,3-dimethylquinoxaline, which is known to undergo deprotonation in the presence of potassium amide and yields 2,3-dipropylquinoxaline after subsequent alkylation.<sup>18</sup> The presence of the active methylene groups in **6** is undoubtedly of synthetic importance, as they offer various possibilities for the functionalization of the thieno[3,4-*b*]quinoxaline core.

We took advantage of **6** and synthesized  $\pi$ -extended dihydrothienoquinoxaline-TTF derivatives **9a** and **9b** by condensation of **6** with 2 equiv of 2-methylthio-1,3-dithiolium salts **10** and **11**, respectively (Scheme 1). The best results were achieved when the condensations were carried out in DMF, in the presence of potassium *tert*-butoxide as the base. Derivatives **9a** and **9b** form green and highly stable microcrystals but decompose slowly in solution, in the presence of air or light.

The synthesis of the more  $\pi$ -extended vinylogues **12a–c** involved the reaction of the diformyl derivative **7** and dithiolium ylide reagents (Scheme 2). Originally, we investigated the use of Wittig-type reactions.<sup>19</sup> The starting phosphonium salt **13** is a stable compound, which is available using a known methodology.<sup>19</sup> The condensation of the dialdehyde **7** with the tributylphosphonium salt **13**, in the presence of triethylamine, leads to the formation of the desired symmetrical product **12a** and also the monoaldehyde **14**. The yields of **12a** and **14** depend greatly on the reaction solvent: in acetonitrile, for instance, the main product was found to be the monocondensation product **14**. In DMF, however, the monoaldehyde was not formed at all, while the biscondensation product **12a** was formed in high yield. The

(10) Hansen, T. K.; Lakshmikantham, M. V.; Cava, M. P.; Becher, J. *J. Chem. Soc., Perkin Trans. 1* **1991**, 2837.

(11) Hansen, T. K.; Lakshmikantham, M. V.; Cava, M. P.; Becher, J. *J. Org. Chem.* **1991**, *56*, 2720.

(12) Lakshmikantham, M. V.; Cava, M. P. *Curr. Sci.* **1994**, *66*, 28.

(13) Hansen, T. K.; Lakshmikantham, M. V.; Cava, M. P.; Niziurski-Mann, R. E.; Jensen, F.; Becher, J. *J. Am. Chem. Soc.* **1992**, *114*, 5035.

(14) Roncali, J. *J. Mater. Chem.* **1997**, *7*, 2307.

(15) Khodorkovsky, V.; Becker, J. Y. In *Organic Conductors, Fundamentals and Applications*; Farges, J. P., Ed.; Marcel Dekker: New York, 1994; Chapter 3, p 75.

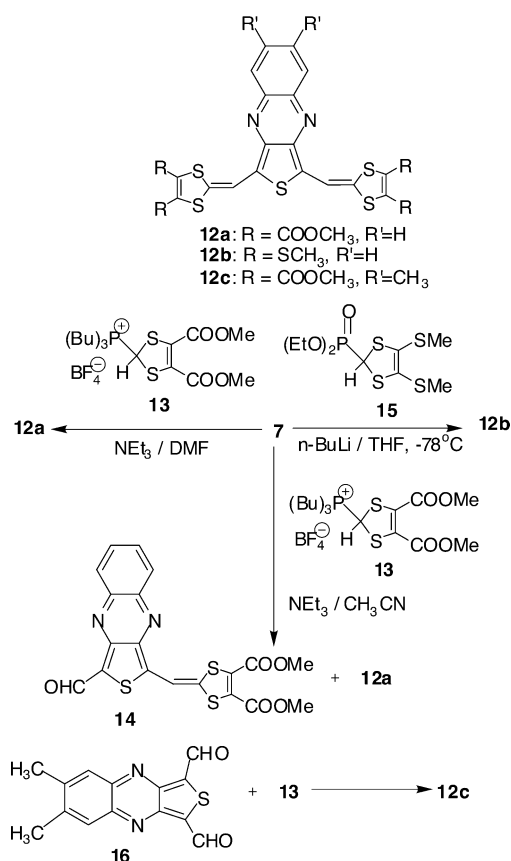
(16) Aqad, E.; Lakshmikantham, M. V.; Cava, M. P. *Org. Lett.* **2003**, *5*, 4089

(17) Pohmer, J.; Lakshmikantham, M. V.; Cava, M. P. *J. Org. Chem.* **1995**, *60*, 8283.

(18) Ogg, R. A., Jr.; Bergstrom, F. W. *J. Am. Chem. Soc.* **1931**, *53*, 1846.

(19) Sato, M.; Gonella, N.; Cava, M. P. *J. Org. Chem.* **1979**, *44*, 930.

## SCHEME 2



best results for the synthesis of **12b** were obtained when we employed a Wittig–Horner-type reaction.<sup>20,21</sup> Thus, the reaction of **7** with the phosphonate **15** afforded the symmetrical product **12b** in high yield. The derivative **12c** was obtained, by full analogy to the synthesis of **12a**, using the known<sup>17</sup> 6,7-dimethyl-1,3-dihydrothieno[3,4-*b*]quinoxaline (**16**) and phosphonium salt **13**. The  $\pi$ -extended TTF analogues **12a–c** were found to be highly stable, both in the solid state and in solution.

**Electronic Absorption Spectra.** The optical absorption spectrum of compound **9a** in CH<sub>2</sub>Cl<sub>2</sub> (Figure 1) contains, besides the absorption bands at 307 ( $\epsilon = 8800$ ), 356 ( $\epsilon = 7800$ ), 440 ( $\epsilon = 18300$ ), 464 ( $\epsilon = 18200$ ) nm, a broad absorption in the range 500–700 nm, centered at 612 nm ( $\epsilon = 7000$ ), with a weak shoulder at 572 ( $\epsilon = 5900$ ) nm. These  $\epsilon$  values are all independent of concentration.

We assign the broad lowest-energy band at 612 nm for **9a** as an intramolecular charge-transfer band (ICT) between the  $\pi$ -extended TTF-donating moiety (a strong electron donor D) and the quinoxaline moiety (a weak-electron acceptor A). The electron-withdrawing effect of the pyrazine ring was best demonstrated by the high reactivity of the methylene groups on **6**.

The ICT-band peak for **9a** ranges from 606 nm in acetonitrile to 616 nm in chlorobenzene (Table 1). This small range indicates that  $\mu_e - \mu_g$ , the difference between the ground-state dipole moment  $\mu_g$  and the excited-state dipole moment  $\mu_e$ , is small. Table 1 also lists various measures for the polarity of the solvents used in this study: the gas-phase dipole moment  $\mu$ , the dielectric constant or relative dielectric permittivity  $\epsilon$ , the refrac-

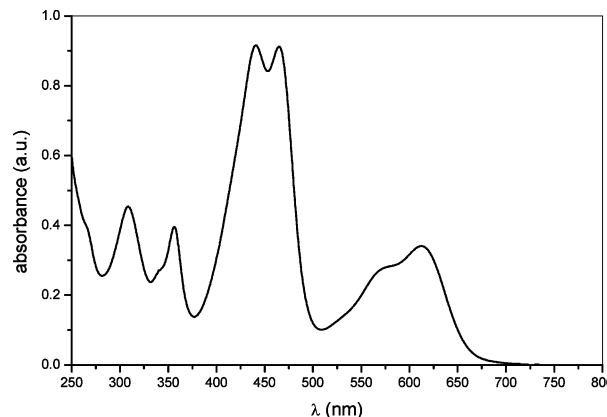


**FIGURE 1.** UV–vis absorption spectrum of compound **9a** in CH<sub>2</sub>Cl<sub>2</sub>.

tive index  $n_D$  (Na D line), the Bayliss–McRae dipolar reaction field factor  $f(e) - f(n_D^2)$ .<sup>22</sup>

$$f(e) - f(n_D^2) = (\epsilon - 1)/(2\epsilon + 1) - (n_D^2 - 1)/(2n_D^2 + 1) \quad (1)$$

and the Reichardt polarity parameter ET.<sup>22</sup> These measures can be used to assess the solvatochromism of the ICT band for compounds **9a,b**, **12a–c**, and **14**. For **9a**, the ICT band maximum depends almost linearly on the solvent refractive index: its value shifts (apparently hypsochromically) from 606 nm in the high-polarity solvent acetonitrile ( $n_D = 1.3441$ ) to 616 nm in the low-polarity solvent chlorobenzene ( $n_D = 1.5248$ ), but the dependence on the other parameters is less clear.

In the absence of specific solvent–solute interactions, solvatochromic shifts can also be described by the equation<sup>23</sup>

$$E = E_{\text{vac}} + Af(n^2) + B[f(\epsilon) - f(n^2)] \quad (2)$$

where  $E$  is the electronic transition energy in a solvent,  $E_{\text{vac}}$  is the electronic transition energy in a vacuum,  $f(x)$  is defined in eq 1,  $A = -1/a^3(K + \mu_e^2 - \mu_g^2)$ ,  $B = -2/a^3\mu_g(\mu_e - \mu_g)$ , and  $K$  is a dispersion term.<sup>23</sup> Although this equation cannot be used explicitly when so many terms (the dispersion term  $K$ , the Onsager cavity radius  $a$ , and the ground- and excited-state dipole moments  $\mu_g$  and  $\mu_e$ ) are unknown, one can assess the solvatochromism by the sign of the parameter  $B$ . A negative  $B$  means<sup>23</sup> that  $\mu_e > \mu_g$  and that the solvatochromism is positive (bathochromism, or red shift).<sup>22</sup> In contrast, a positive  $B$  means<sup>23</sup> that  $\mu_e < \mu_g$  and that the solvatochromism is negative (hypsochromism, or blue shift).<sup>22</sup> A least-squares fitting for **9a** afforded  $E_{\text{vac}} = 17429 \text{ cm}^{-1}$  ( $\lambda_{\text{vac}} = 573.8 \text{ nm}$ ),  $A = -3839$ , and  $B = -196$ . Table 1 also lists the calculated absorption wavelengths for **9a**, calculated using eq 2. The small, but negative, value of  $B$  means that the dipole moment change upon excitation is small, in the direction  $\mu_e > \mu_g$ , and, therefore, that the solva-

(20) Akiba, K.; Ishikawa, K.; Inamoto, N.; *Bull. Chem. Soc. Jpn.* **1978**, *51*, 2674.

(21) Yamashita, Y.; Kobayashi, Y.; Miyashi, T. *Angew. Chem., Int. Ed.* **1989**, *28*, 1052.

(22) Reichardt, C. *Solvents and Solvent Effects in Organic Chemistry*, 2nd ed.; VCH: Weinheim, 1990.

(23) Amos, A. T.; Burrows, B. L. *Adv. Quantum Chem.* **1973**, *7*, 289–313.

**TABLE 1.** Longest Wavelength Absorption (Intramolecular Charge Transfer, ICT) Band Maxima  $\lambda_{\text{max}}$  of **9a,b**, **12a–c**, and **14** in Various Solvents, Correlated with Polarity Data for These Solvents [Dipole Moment  $\mu$ , Dielectric Constant (Relative Dielectric Permittivity)  $\epsilon$ , Refractive Index  $n_D$  (Na D line), Bayliss–McRae Dipolar Reaction Field Factor ( $\epsilon - 1$ )/( $2\epsilon + 1$ ) - ( $n_D^2 - 1$ )/( $2n_D^2 + 1$ ) and Reichardt Polarity Parameter  $E_T$ ]<sup>a</sup>

solvent	dipole moment $\mu/D$	dielectric constant $\epsilon$	refractive index $n_D$	Bayliss–McRae factor	Reichardt polarity $E_T$	exptl ICT maxima ( $\lambda_{\text{max}}/\text{nm}$ )					calcd ( $\lambda_{\text{max}}/\text{nm}$ )	
						<b>9b</b>	<b>12a</b>	<b>12b</b>	<b>12c</b>	<b>14</b>	<b>9a</b>	
CH <sub>3</sub> CN	3.92	37.5	1.3441	0.1143	0.460	603	785	790	766	666	606	606.2
acetone	2.88	20.56	1.3586	0.0984	0.355	604	773	786	760	665	607	606.8
CH <sub>2</sub> Cl <sub>2</sub>	1.60	8.93	1.4242	0.0549	0.309	600	802	807	775	670	612	610.5
toluene	0.36	2.38	1.4969	-0.1242	0.099	601	808	807	782	671	612	612.0
C <sub>6</sub> H <sub>5</sub> Cl	1.69	5.62	1.5248	0.0148	0.188	607	809	809	784	673	616	616.0

<sup>a</sup> The absorption maxima calculated after fitting the experimental data for **9a** to eq 2 are listed in the last column.

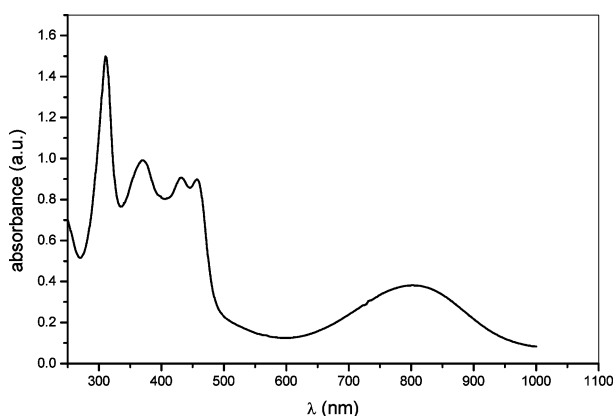


**FIGURE 2.** UV–vis absorption spectrum of compound **12a** in CH<sub>2</sub>Cl<sub>2</sub>.

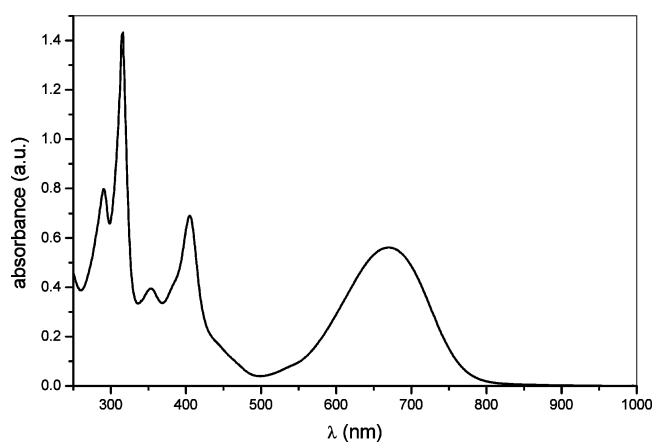


**FIGURE 3.** UV–vis absorption spectrum of compound **14** in CH<sub>2</sub>Cl<sub>2</sub>.

tochromism for **9a** is positive (bathochromic shift). Similar results were obtained for other derivatives of the series.

Similar optical absorption features were observed for the tetramethylthio derivative **9b**, for which the ICT band is located at 600 nm ( $\epsilon = 7100$ ) in methylene chloride (versus 612 nm for **9a** in the same solvent). Thus, different substitutions at the peripheral carbon atoms of 1,3-dithiole heterocycles affect moderately the position of the ICT band. However, a definite solvatochromic trend for **9b** could not be determined as clearly as it was for compound **9a**.

The UV–vis absorption spectrum of the more  $\pi$ -extended TTF derivative **12a** in CH<sub>2</sub>Cl<sub>2</sub> contains, besides the absorption maxima at 310 ( $\epsilon = 18800$ ), 371 ( $\epsilon =$

11900), 430 ( $\epsilon = 11400$ ), and 457 ( $\epsilon = 11100$ ) nm, a broad band at 802 nm ( $\epsilon = 5800$ ) (Figure 2), which is characteristic for an ICT interaction. The molar absorptivities of all these bands are also independent of concentration. Again, the position of the ICT band depends monotonically on the solvent refractive index  $n_D$ , which is exemplified by the large shift from 785 nm in acetonitrile ( $n_D = 1.3441$ ) to 809 nm in chlorobenzene, ( $n_D = 1.5248$ ).

The UV–vis absorption spectrum of derivative **12b**, bearing the methylthio groups at the peripheral carbon atoms of the 1,3-dithiole heterocycle, has absorption features similar to those of the tetramethoxycarbonyl derivative **12a**. The ICT band (in methylene chloride) of **12b** is red-shifted by only 5 nm, compared to **12a**. As expected, the substitution at the benzene ring of the electron-accepting moiety with the electron-donating methyl groups, as in **12c** ( $\lambda_{\text{ICT}} = 775$  nm in CH<sub>2</sub>Cl<sub>2</sub>,  $\epsilon = 5800$ ), brings about a blue-shift of 27 nm, compared to **12a** in the same solvent. These observations indicate the sensitivity of the location of the ICT band to the nature of the substituent on peripheral carbon atoms. Similar to **12a**, the ICT band maxima of **12b** and **12c** are strongly dependent on the solvent refractive index.

The UV–vis spectrum of the purple-colored monoaldehyde derivative **14** in CH<sub>2</sub>Cl<sub>2</sub> (Figure 3) contains, besides absorptions at 290 ( $\epsilon = 19800$ ), 316 ( $\epsilon = 35500$ ), 353 ( $\epsilon = 9800$ ), and 405 ( $\epsilon = 17300$ ) nm, a broad absorption band with  $\lambda_{\text{max}} = 670$  nm ( $\epsilon = 14500$ ). We also attribute this last band to the intramolecular electronic interaction. The structure of **14** bears a delocalized  $\pi$ -electron system, which is capped with end-groups of disparate electron affinities (1,3-dithiole-2-ylidene is electron-donating, while formyl is electron-accepting). Therefore, formally, compound **14** resembles chemical structures that are polarizable in an asymmetric manner (push–pull structures). The ICT band maxima of push–pull structures typically strongly depend on solvent polarity. However, the ICT band maximum of **14** does not depend monotonically on the usual measures<sup>24</sup> of solvent polarity, but again, like in the case of derivatives **9** and **12**, it depends almost monotonically on the refractive index of the solvents.

In summary, the wavelengths of ICT band maxima  $\lambda_{\text{max}}$  for compounds **9a,b**, **12a–c**, and **14** increase with increasing refractive index. As the solvent polarity increases, the ICT bands undergo a blue shift (hypsochromism, or negative solvatochromism) in all these

(24) Bryce, R. M.; Coffin, M. A.; Clegg, W. *J. Org. Chem.* **1992**, *57*, 1696.

compounds. However, as discussed above, the small observed hypsochromic shift for **9a** becomes a calculated bathochromic shift (positive solvatochromism) when eq 2 is used. In calculations shown below, the excited-state dipole moment for a compound related to the above is larger than the ground-state moment: this also supports bathochromism for this class of compounds.

**Electrochemistry.** The redox properties of the new compounds were studied by cyclic voltammetry. For comparisons, the cyclic voltammograms (CVs) of parent TTF, tetramethyl-TTF, and tetramethylthio-TTF were measured under the same experimental conditions (SCE reference electrode). The results are collected in Table 2.

The CVs of compound **9a** and **9b** exhibit, on anodic scanning, two reversible one-electron oxidation steps, which correspond to the formation of stable cation radicals (**9a'**, **9b'**) and dications (**9a''** and **9b''**), respectively (Scheme 3). On cathodic scanning from 0 to  $-1.75$  V, the CVs for **9a** and **9b** show no peaks. We attributed the lack of cathodic response to the relatively weak electron-accepting ability of the quinoxaline ring, which is further diminished by the ICT interaction. Judging from the anodic waves, it appears that the  $\pi$ -extended TTF derivatives **9a** and **9b** maintain their expected electron-donating characteristics: (1) compound **9a**, bearing four strong donating methyl groups on the peripheral carbon atoms of the 1,3-dithiole heterocycle, is a stronger donor than **9b**; (2) **9a** and **9b** are more electron-donating than their simple TTF analogues. In particular, the first oxidation potential of **9a** is lower by 0.16 V than that of tetramethyl-TTF, while the first oxidation potential of **9b** is lower by 0.12 V than that of the parent TTF, and is lower by 0.30 V than that of tetramethylthio-TTF. The relatively strong donating abilities of **9a** and **9b** is attributed to the generation of the highly stable cation radicals of the general structures **9a'** and **9b'**, which bear the favored heteroaromatic *o*-quinonoid thieno[3,4-*b*]quinoxaline fragment and two heteroaromatic 1,3-dithiole moieties (Scheme 3). The  $\Delta E_{\text{ox}}$  values for **9a** and **9b** are larger than those observed for TTF derivatives. This is unusual, since closely related  $\pi$ -extended structures exhibit significantly low  $\Delta E$  values.<sup>15</sup> Interestingly enough, this observation was predicted by the theoretical calculations performed for a model compound (see below), which indicated a relatively small Coulomb repulsion for the dication oxidation state of this system.

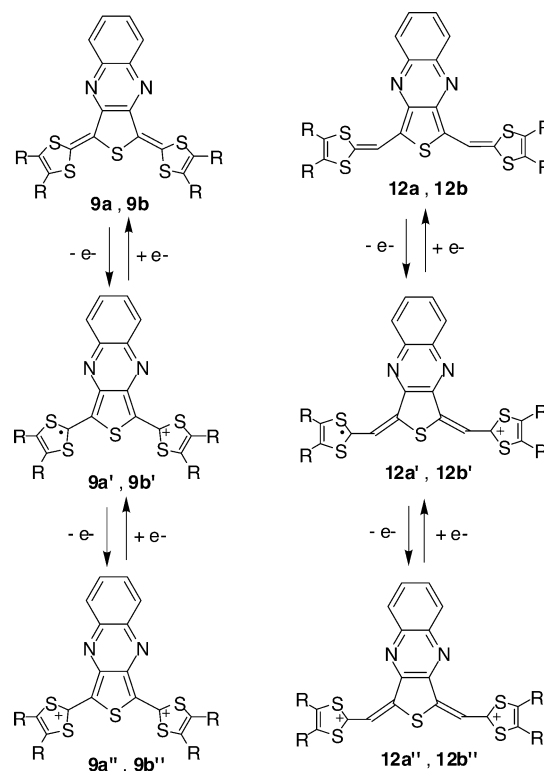
**TABLE 2.** Redox Potentials (First and Second Oxidation Potentials  $E^1_{\text{ox}}$  and  $E^2_{\text{ox}}$ , First and Second Reduction Potentials  $E^1_{\text{red}}$  and  $E^2_{\text{red}}$ , and Difference  $\Delta E = E^2 - E^1$ ) for the New and Reference Compounds<sup>a</sup>

compd	$E^1_{\text{ox}}$ (V)	$E^2_{\text{ox}}$ (V)	$E^1_{\text{red}}$ (V)	$E^2_{\text{red}}$ (V)	$\Delta E_{\text{ox}}$ (V)
<b>9a</b>	0.09	0.51			0.42
<b>9b</b>	0.23	0.64			0.41
<b>12a</b>	0.38	0.62	$-1.08^b$		0.24
<b>12b</b>	0.29	0.49	$-0.96^b$		0.20
<b>12c</b>	0.35	0.57	$-1.23^b$		0.22
<b>14</b>	0.84		$-0.58^b$		
TTF	0.33	0.69			0.36
tetramethyl-TTF	0.25	0.61			0.35
tetramethylthio-TTF	0.51	0.77			0.26
<b>7</b>			$-0.22$	$-0.72$	0.50

<sup>a</sup>  $5 \times 10^{-4}$  M in  $\text{CH}_2\text{Cl}_2$ ,  $\text{Bu}_4\text{NPF}_6$  supporting electrolyte, SCE reference electrode, Pt working electrode, 100 mV/s scan rate.

<sup>b</sup> Two-electron irreversible process.

### SCHEME 3

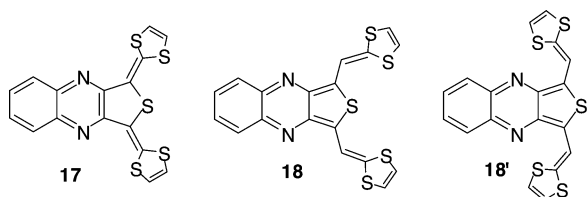


The CVs of the vinyllogs **12a–c** exhibit two one-electron waves on anodic scanning, corresponding to the formation of the cation radical and dication, respectively. As expected, these compounds exhibit strong electron-donating abilities, compared to their TTF analogues, as is evident from the significantly lower oxidation potential of the tetramethylthio derivative **12b**, compared to tetramethylthio-TTF. As expected, compound **12a**, with four carbomethoxy groups, exhibits a weaker electron-donating ability, compared to **12b**. Interestingly, methyl substitution on the 6- and 7-positions of the benzene ring does not affect largely the donating properties of these compounds, as evident from the very small cathodic shift between **12a** and **12c** (0.02 V). The difference between the two-oxidation potentials ( $\Delta E$ ) for derivatives **12a–c** is in the range 0.20–0.24 V, which is significantly smaller than that of TTF, but is similar to the  $\Delta E$  for other reported tetrathiafulvalene systems with heterocyclic spacer groups.<sup>13</sup>

As has been already shown,<sup>15</sup> small  $\Delta E$ s are associated with a decreased Coulomb repulsion in the dicationic state of such molecular systems. Hence, among other possible structures, which might describe the bonding nature of the dications derived from **12a–c**, structures **12a''–c''** are likely to be very favored, since they account for a small Coulomb repulsion (Scheme 3).

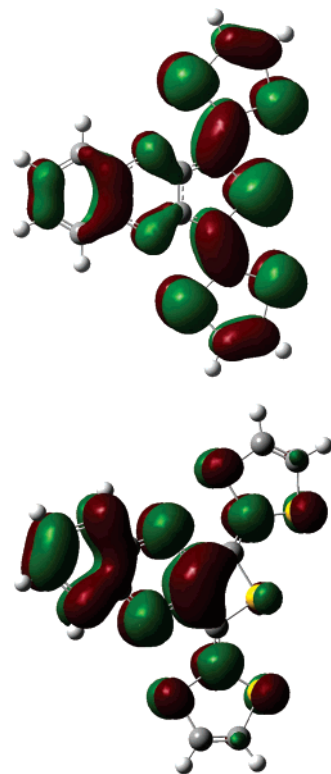
The electron-accepting properties of **12a–c** are seen on their CVs. On cathodic scanning, compounds **12a–c** exhibit two-electron, mostly irreversible, reduction waves. The reduction potential values ( $-0.96$  V for **12b** and  $-1.23$  V for **12c**) indicate that the electron-accepting abilities of these compounds are stronger than those of **9**. It will be interesting to compare the reduction potentials of **12a–c** with those of the parent thieno[3,4-*b*]quinoxaline (**8**). However, the CV of **8** gave inconsistent

CHART 2



results due to its instability under the experimental conditions. On the other hand, the CV of the stable diformyl derivative **7** exhibits two reversible one-electron reduction steps, at  $-0.22$  and  $-0.72$  V, respectively. These values are similar to those for the recently reported selenium analogue<sup>16</sup> of **7** and present the first experimental measure for the electron-accepting ability of stable thieno[3,4-*b*]quinoxaline derivatives. Compound **14**, in which the thieno[3,4-*b*]quinoxaline core is capped on one end with a formyl electron-withdrawing group and, at the other end, with a 1,3-dithiole-2-ylidene electron-donating group, exhibits only a single two-electron reduction wave at  $-0.58$  V. The conjugated annelation of the “electron-accepting” thieno[3,4-*b*]quinoxaline core with the strong electron-donating 1,3-dithiol-2-ylidene moieties, as in **12a–c**, and **14**, leads to a new molecular system, with an intramolecular electronic interaction, and, as a consequence, to a large decrease in the electron-accepting ability of the thieno[3,4-*b*]quinoxaline core, and to the coalescence of the two one-electron reduction waves into a single two-electron wave.

**Quantum Mechanical Calculations.** The UV–vis and electrochemical studies of the newly synthesized  $\pi$ -extended TTFs indicated clearly the presence of the donor–acceptor intramolecular CT interaction. To get deeper insight into the nature of this interaction, we performed quantum chemical calculations<sup>25</sup> for the parent compounds **17** and **18** (Chart 2). Preliminary calculations on semiempirical levels (AM1, PM3) showed that isomer **18** is about 10 kcal/mol more stable than **18'**. Therefore, a detailed DFT study has been done for derivatives **17** and **18**. For comparison, the calculations were also performed for TTF and *p*-benzoquinone (PBQ). All geometries were optimized using the B3LYP/6-31G(d) model chemistry. A visual examination of HOMOs and LUMOs for both compounds, given in Figures 4 and 5, shows that the optical HOMO–LUMO transition should have a charge-transfer nature, with the electron density shifting mostly from the electron-donat-



**FIGURE 4.** Atom-centered electron amplitudes (molecular orbital coefficients) for HOMO (upper diagram) and LUMO (lower diagram) of **17**.

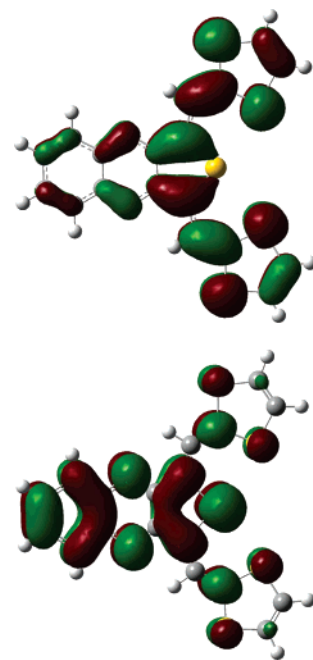


**FIGURE 5.** Atom-centered electron amplitudes (molecular orbital coefficients) for HOMO (upper diagram) and LUMO (lower diagram) of **18**.

ing 1,3-dithiole moieties to the accepting quinoxaline (**17**) and thieno[3,4-*b*]quinoxaline (**18**) moieties, although the overall change in the electron density distribution is not large. The calculated dipole moments for **17** (at the CIS/B3LYP/6-311+(2d,p) level) were 0.86 and 3.34 D for the ground state and the first excited state, respectively

(25) Frisch, M. J.; Trucks, G. W.; Schlegel, H. B.; Scuseria, G. E.; Robb, M. A.; Cheeseman, J. R.; Montgomery, J. A. Jr.; Vreven, T.; Kudin, K. N.; Burant, J. C.; Millam, J. M.; Iyengar, S. S.; Tomasi, J.; Barone, V.; Mennucci, B.; Cossi, M.; Scalmani, G.; Rega, N.; Petersson, G. A.; Nakatsuji, H.; Hada, M.; Ehara, M.; Toyota, K.; Fukuda, R.; Hasegawa, J.; Ishida, M.; Nakajima, T.; Honda, Y.; Kitao, O.; Nakai, H.; Klene, M.; Li, X.; Knox, J. E.; Hratchian, H. P.; Cross, J. B.; Adamo, C.; Jaramillo, J.; Gomperts, R.; Stratmann, R. E.; Yazyev, O.; Austin, A. J.; Cammi, R.; Pomelli, C.; Ochterski, J. W.; Ayala, P. Y.; Morokuma, K.; Voth, G. A.; Salvador, P.; Dannenberg, J. J.; Zakrzewski, V. G.; Dapprich, S.; Daniels, A. D.; Strain, M. C.; Farkas, O.; Malick, D. K.; Rabuck, A. D.; Raghavachari, K.; Foresman, J. B.; Ortiz, J. V.; Cui, Q.; Baboul, A. G.; Clifford, S.; Cioslowski, J.; Stefanov, B. B.; Liu, G.; Liashenko, A.; Piskorz, P.; Komaromi, I.; Martin, R. L.; Fox, D. J.; Keith, T.; Al-Laham, M. A.; Peng, C. Y.; Nanayakkara, A.; Challacombe, M.; Gill, P. M. W.; Johnson, B.; Chen, W.; Wong, M. W.; Gonzalez, C.; Pople, J. A. *Gaussian 03, Revision B.05*; Gaussian, Inc.: Pittsburgh, PA, 2003.

**TABLE 3.** Calculated Ionization Potentials (IP) and Electron Affinities (EA) for **17** and **18** and the Reference Compounds Tetrathiafulvalene (TTF, **1**) and *p*-Benzoquinone (PBQ)<sup>15</sup>

compd	IP (eV)	EA (eV)
<b>17</b>	5.99	1.13
<b>18</b>	5.48	1.75
TTF	6.25 (expt 6.70–6.92)	
PBQ		2.12 (expt 1.85)

(this would suggest that **17** is bathochromic, or should have positive solvatochromism, as was found by applying eq 2 to the ICT bands of compound **9a**). The dipole moments of donor/acceptor-substituted aromatics, which exhibit moderate to strong positive solvatochromism (bathochromism), are considerably larger, e.g., 3–5 and 18–22 D in the ground and excited states, respectively.<sup>26</sup> Therefore, in the absence of strong electron-density shifts upon excitation, the polar interactions with a solvent will be small. The nonplanar conformers of **18** in solution should possess even smaller ground and excited-state dipole moments. Therefore, the major factor determining the energy shifts of the HOMO–LUMO transition in solution should be the refractive index, rather than the dielectric constant of the solvent.

Interestingly, the sulfur atom of the thiophene moiety contributes considerably to the HOMO of **17**, whereas the corresponding coefficient in the HOMO of **18** is zero, and the HOMO of the latter resembles the HOMOs of other TTF vinyls of type **4**. The difference between derivatives **17** and **18** can thus be identified as follows. The electron-donating moiety of **17** is the 2,2'-[thiodi(methylidene)]bis-1,3-dithiole fragment, while the electron-accepting moiety is the quinoxaline fragment: molecule **17** can therefore be defined as a D- $\pi$ -A type structure. The electron-donating moieties of **18** are both 1,3-dithiole-2-ylidene fragments, while the electron-accepting moiety is the thieno[3,4-*b*] fragment; molecule **18** can thus be defined as a D- $\pi$ -A- $\pi$ -D type structure. One can expect that it will be more difficult to oxidize the cation radical of **17**, than that of **18**, because the Coulomb repulsion for the dication of **18** will be smaller, which is in good agreement with the observed  $\Delta E_{ox}$  for derivatives **9a** and **9b**. Calculations of the electronic absorption spectra of both compounds have been made by the time-dependent (TD) B3LYP/6-311+G(2d,p) method. The longest-wavelength absorption band for both derivatives appeared to be essentially due to a HOMO–LUMO transition, 570 nm for **17** and 910 nm for **18**, numbers which are in good agreement with experiment. We also calculated the ionization potentials (IP) and electron affinities (EA) for **17**, as the difference between the energies of the neutral, cation radical, and anion radical species at the B3LYP/6-311+G(2d,p) level. The corresponding data for **17**, **18**, TTF, and PBQ are given in Table 3.

The derivatives **17** and **18** are both predicted to be better donors than TTF, in agreement with experimental CV potentials. The IP of derivative **18** is apparently overestimated; however, unlike **17**, compound **18** can exist in solution as a mixture of several nonplanar conformers, and the decreased conjugation between the

two dithiole moieties should considerably diminish the electron-donating ability of **18**, without affecting strongly the rigid electron-accepting moiety. The calculated EA values are also in agreement with experiment: whereas **17** is much weaker acceptor than PBQ, the difference between the EAs of PBQ and **18** amounts to just 0.37 eV.

**Summary and Conclusions.** The present work describes the synthesis of new TTF architectures in which (1) two 1,3-dithiole moieties are separated by the weak electron-accepting quinoxaline moiety, exemplified by derivative **9a** and **9b**, and (2) two 1,3-dithiole-2-ylidene moieties are separated by the electron-accepting thieno[3,4-*b*]quinoxaline bridge, exemplified by derivatives **12a–c**. The newly prepared compounds are D- $\pi$ -A and D- $\pi$ -A- $\pi$ -D molecular systems, and, as such, they exhibit through-bond intramolecular charge-transfer interactions, which were reproduced by theoretical calculations and confirmed by UV–vis spectroscopy and cyclic voltammetry measurements. To the best of our knowledge, the potential of quinoxalines as an electroactive electron-accepting building block for new materials with ICT interaction was demonstrated here for the first time.

## Experimental Section

4,5-Dimethyl-2-methylthio-1,3-dithiolium salt **10** was prepared from 4,5-dimethyl-1,3-dithiol-2-thione and a large excess of methyl iodide in dry acetonitrile. The salt **11**<sup>11</sup> was prepared from 4,5-dimethylthio-1,3-dithiol-2-thione according to a general procedure. The phosphonium salt **13**,<sup>19</sup> phosphonate **15**,<sup>10</sup> 1,3-dihydrothieno[3,4-*b*]quinoxaline (**6**),<sup>17</sup> 1,3-diformylthieno[3,4-*b*]quinoxaline (**7**),<sup>17</sup> and 6,7-dimethyl-1,3-diformylthieno[3,4-*b*]quinoxaline (**16**)<sup>17</sup> were prepared using literature procedures.

**1,3-Bis(4,5-dimethyl-1,3-dithiol-2-ylidene)-1,3-dihydrothieno[3,4-*b*]quinoxaline (9a).** 1,3-Dithiolium salt **10** (2 g, 6.58 mmol) and 1,3-dihydroquinoxaline (**6**) (0.50 g, 2.65 mmol) were dissolved in 10 mL of dry DMF. To the stirred solution was added *t*-BuOK (0.60 g, 5.35 mmol), and the stirring was continued for 15 h. Water (25 mL) was added, and the resulting precipitated solid was collected and dried. Repeated recrystallization of the precipitate from pyridine gave analytically pure **9a** as green microcrystals. Compound **9a** decomposes slowly in solutions, it can be kept in pyridine in the dark and under inert atmosphere for several weeks. It is, however, stable in the solid state: yield 0.95 g (80%); mp 209–212 °C dec; <sup>1</sup>H NMR (CDCl<sub>3</sub>)  $\delta$  2.14 (s, 6H), 2.16 (s, 6H), 7.52 (dd, *J* = 7.1, 3.1 Hz, 2H), 7.98 (dd, *J* = 7.1, 3.1 Hz, 2H); MS *m/e* (relative intensity) 444.99 (M<sup>+</sup>, 100), 281.03 (10) 259.87 (20), 221.92 (10). Anal. Calcd for C<sub>20</sub>H<sub>16</sub>N<sub>2</sub>S<sub>5</sub>: C, 54.02; H, 3.63; N, 6.30; S, 36.05. Found: C, 53.96; H, 3.90; N, 6.29; S, 35.80.

**1,3-Bis[(4,5-bis(methylthio)-1,3-dithiol-2-ylidene)-1,3-dihydrothieno[3,4-*b*]quinoxaline (9b).** Compound **9b** was obtained by analogous procedure for the preparation of **9a**, starting from **6** and the 1,3-dithiolium salt **11**. Similar to **9a**, compound **9b** decomposes slowly in solutions, it can be kept in pyridine in the dark and under inert atmosphere for several weeks. It is, however, stable in the solid state: yield 84%; mp 221–224 °C dec; <sup>1</sup>H NMR (CDCl<sub>3</sub>)  $\delta$  2.51 (s, 6H), 2.54 (s, 6H), 7.55 (dd, *J* = 7.3, 3.0 Hz, 2H), 7.93 (dd, *J* = 7.3, 3.0 Hz, 2H). MS *m/e* (relative intensity) 571.88 (M<sup>+</sup>, 100), 523.54 (10) 476.97 (20), 321.92 (10). Anal. Calcd for C<sub>20</sub>H<sub>16</sub>N<sub>2</sub>S<sub>9</sub>: C, 41.93; H, 2.81; N, 4.89; S, 50.37. Found: C, 41.67; H, 2.90; N, 4.69; S, 49.77.

**Reaction of 1,3-Diformylthieno[3,4-*b*]quinoxaline (7) with Phosphonium Salt 13 in Acetonitrile.** The phosphonium salt **15** (1.1 g, 2.36 mmol) and 0.25 g of the diformyl derivative **7** (1.0 mmol) were dissolved in 7 mL of dry acetonitrile. To the stirred solution was added 0.20 mL of

(26) Shumalekshmy, S.; Gopidas, K. R. *J. Phys. Chem. B* **2004**, *108*, 3705.

triethylamine, and stirring was continued for 5 h. Water (10 mL) was added, and the precipitated solid was collected and dried. The precipitate was dissolved in a minimal amount of methylene chloride and chromatographed through a silica gel column. The first purple fraction of the monocondensation product **14** was eluted with methylene chloride/hexane (1:1). The second fraction of the yellow bis-condensation product **9a** was eluted with  $\text{CH}_2\text{Cl}_2$ . Evaporation of solvents from the first fraction, and subsequent recrystallization from acetonitrile, gave **14** as deep-blue microcrystals (0.28 g, 62%). Evaporation of solvents from the second fraction, and subsequent recrystallization from chloroform/hexane (1:1) gave compound **12a** (0.18 g, 27%).

**Tetramethyl-2,2'-[thieno[3,4-*b*]quinoxaline-1,3-diyl-di(methylidene)]bis(1,3-dithiole-4,5-dicarboxylate) (12a):** mp 242 °C;  $^1\text{H}$  NMR ( $\text{CDCl}_3$ )  $\delta$  3.91 (s, 6H), 3.95 (s, 6H), 7.61 (d,  $J = 4.8$  Hz, 2H), 7.89 (s, 2H), 7.96 (d,  $J = 4.8$  Hz, 2H); MS *m/e* (relative intensity) 644.26 (11), 642.0 (100), 587.83 (64), 338.94 (34), 336.94 (58). Anal. Calcd for  $\text{C}_{26}\text{H}_{18}\text{N}_2\text{O}_8\text{S}_5$ : C, 48.28; H, 2.81; N, 4.33; S, 24.79. Found: C, 47.95; H, 3.00; N, 4.30; S, 24.04.

**Reaction of 1,3-Diformylthieno[3,4-*b*]quinoxaline (7) with Phosphonium Salt 15 in DMF.** The phosphonium salt **15** (1.1 g, 2.36 mmol) and 0.25 g of the diformyl derivative **11** (1.0 mmol) were dissolved in 7 mL of dry DMF. To the stirred solution were added 0.20 mL of triethylamine, and stirring was continued for 5 h. Water (10 mL) was added, and the precipitated solid was collected and dried. The precipitate was dissolved in a minimal amount of methylene chloride and passed through a short silica gel column. Evaporation of the solvent, and subsequent recrystallization from chloroform/hexane (1:1), gave compound **9a** (0.54 g, 81%).

**1,3-Bis{[4,5-bis(methylthio)-1,3-dithiol-2-ylidene]-methyl}thieno[3,4-*b*]quinoxaline (12b).** The phosphonate **15** (0.76 g, 2.27 mmol) was dissolved in 10 mL of dry THF under an inert atmosphere. The solution was cooled to  $-78$  °C in a dry ice/acetone bath. A solution of *n*-BuLi in hexane (1.5 mL, 2.40 mmol; 1.6 M solution) was added dropwise. Five minutes after the addition was completed, a solution of **7** (0.25

g, 1.0 mmol) in 20 mL of dry THF was added over a period of 20 min. The cooling bath was removed, and the reaction mixture was stirred at room temperature for 2 h. It was then poured into 50 mL of water. The resulting precipitate of crude **12b** was collected and dried. The crude product was dissolved in a minimal amount of methylene chloride and passed through a short column of silica gel (methylene chloride eluent). Evaporation of the solvent and subsequent recrystallization from toluene gave analytically pure product: yield 0.52 g, 84%; mp 236 °C;  $^1\text{H}$  NMR ( $\text{CDCl}_3$ )  $\delta$  2.54 (s, 6H), 2.55 (s, 6H), 7.74 (d,  $J = 4.8$  Hz, 2H), 7.87 (s, 2H), 8.02 (d,  $J = 4.8$  Hz, 2H); MS *m/e* (relative intensity) 597.90 (100), 550.72 (34), 456.01 (40), 321 (10), 298 (63). Anal. Calcd for  $\text{C}_{22}\text{H}_{18}\text{N}_2\text{S}_9$ : C, 44.11; H, 3.03; N, 4.68; S, 48.18. Found: C, 44.34; H, 3.09; N, 4.42; S, 48.15.

**Tetramethyl 2,2'-[(6,7-dimethylthieno[3,4-*b*]quinoxaline-1,3-diyl)di(methylidene)]bis(1,3-dithiole-4,5-dicarboxylate) (12c)** was obtained by an analogous procedure as for the preparation of **12a**, starting from **16** and the phosphonium salt **13** in DMF: yield 88%; mp 221–222 °C;  $^1\text{H}$  NMR ( $\text{CDCl}_3$ )  $\delta$  2.47 (s, 6H), 3.80 (s, 6H), 3.90 (s, 6H), 7.70 (s, 1H), 7.85 (s, 1H); MS *m/e* (relative intensity) 674.00 ( $\text{M}^+$ , 100), 617, 02 (23), 435.98 (55), 369.68 (80). Anal. Calcd for  $\text{C}_{26}\text{H}_{18}\text{N}_2\text{O}_8\text{S}_5$ : C, 49.84; H, 3.29; N, 4.15; S, 23.76. Found: C, 49.64; H, 3.29; N, 4.02; S, 23.36.

**Dimethyl 2-[(3-formylthieno[3,4-*b*]quinoxalin-1-yl)-methylene]-1,3-dithiole-4,5-dicarboxylate (14):** mp 252 °C;  $^1\text{H}$  NMR ( $\text{CDCl}_3$ )  $\delta$  3.96 (s, 3H), 3.98 (s, 3H), 7.69 (m, 1H), 7.78 (m, 1H), 8.07 (t,  $J = 6.8$  Hz, 2H), 8.27 (s, 1H), 10.77 (s, 1H); MS *m/e* (relative intensity) 443.94 ( $\text{M}^+$ , 100), 415.92 (31), 356.93 (14), 273.90 (81), 241.94 (49), 197.95 (51). Anal. Calcd for  $\text{C}_{19}\text{H}_{12}\text{N}_2\text{O}_5\text{S}_3$ : C, 51.34; H, 2.72; N, 6.30; S, 21.64. Found: C, 51.45; H, 3.00; N, 6.30; S, 21.62.

**Acknowledgment.** The work in Alabama was supported by the United States National Science Foundation (Grant No. DMR-00-95215).

JO0489317